Research Article

Characteristic Analysis and Simulated Test of Hybrid Bearing with the Introduction of Piezoelectric Controller

Runlin Chen,[1] Wu Ouyang,[2] Zhaoyang Shi,[1] Yangyang Wei,[1] and Xiaoyang Yuan[1]

[1]*Key Laboratory of Education Ministry for Modern Design and Rotor-Bearing System, Xi'an Jiaotong University, Xi'an 710049, China*
[2]*School of Energy and Power Engineering, Wuhan University of Technology, Wuhan 430063, China*

Correspondence should be addressed to Xiaoyang Yuan; xyyuan@mail.xjtu.edu.cn

A novel hybrid bearing with the introduction of piezoelectric controller and tilting pads to control vibration actively is proposed in this paper, and the feasibility of this scheme is verified by theoretical calculation and experimental data. This scheme can control the vibration of bearing actively by using the electromechanical characteristics of piezoelectric ceramic transducer (PZT) components. The static internal character of PZT and static external characteristic of piezoelectric control component are analyzed, and the calculation equations of preload coefficient and driving force of the new bearing are given. The simulation setup of the new bearing is designed and developed. The data representing the relationship of displacement of pad pivot, driving force, voltage, and the simulation stiffness of liquid film are obtained in the test, and the feature parameters of piezoelectric control component are amended to analyze the relationship between preload coefficient of the bearing and driving voltage. The proposed new bearing has the function of controlling preload actively. The theoretical and experimental research results provide essential guidance for the detail design of this new bearing and also provide a new idea for the vibration control of high speed rotor systems.

1. Introduction

The liquid hybrid bearing has the advantage of hydrodynamic bearing and hydrostatic bearing. On the one hand, the hydrostatic pressure avoids the dry friction that easily appears in the process of low speed and startup of hydrodynamic bearing. On the other hand, the composite structure of deep cavity and shallow recess in most hybrid bearing can significantly improve the carrying capacity [1]. Besides that, the high-pressure oil film has errors averaging effect on the rotor [2]. The hybrid bearing is widely used in high speed spindles and precision machine tools because of these superiorities. With the development of equipment in aviation and energy sectors towards the high accuracy, the rotation accuracy of spindle is required to be nanoscale [3]. These demands are no longer satisfied by the traditional structures and design methods.

In order to improve the rotation accuracy of spindle, the domestic and foreign scholars have made various attempts; the main methods can be concluded as static force methods and dynamic force methods. The static force methods are

that the antijamming capability to external load is enhanced by improving the bearing film stiffness, which is often implemented by increasing oil pressure, optimizing the cavity structure [4–6], or using film feedback throttle [7]. But there are certain limitations in these methods, such as high energy consumption and high requirements of processing or installation. So, the technology of tilting pad is introduced into hybrid bearing. A typical structure of hybrid tilting pad bearings is proposed since 1980s. One or several oil pockets are set on the surface of tilting pads. At first, this technology is mostly applied in tilting pad thrust bearing, and the hydrostatic pressure is used for a oil lift system [8–10]. Then the technology of high-pressure injection pockets is used for tilting pad journal bearing. But the hydrodynamic pressure only works in the startup and stop phase to lift the rotor [11]. When the rotation speed raises up, the high-pressure oil will be shut down. The experimental results show that the damping and logarithmic decrement are small at working speed, which are the instability factors [12, 13]. According to the engineering experience, the vibration will be excited when the hydrostatic pressure is still kept at high speed,

especially when the oil supply pressure is high. The preload coefficients of tilting pads are important for improving the bearing stiffness. The elastic and damped pivots of tilting pad journal bearing can change the stiffness to suppress the vibration of rotor [14–16]. But these methods or structures could not change the bearing performance actively.

The dynamic force methods are that the vibration response is controlled by imposing an opposite-direction dynamic force to the external exciting force. But there are few related research results. The main methods are using electromagnetic bearing or piezoelectric actuator. The acceleration feed-forward method is proposed to reduce the excited response of impact vibration and forced vibration on the rotor [17, 18]. In fact, the input-output relationship of control system in electromagnetic bearing cannot be exactly expressed by transfer function, which brings difficulties to design and accuracy control. Moreover, electromagnetic devices are combined with hydrodynamic bearing to resist the unbalanced force, which is a vibration reduction method of online dynamic balancing [19]. Balini et al. [20] designed and implemented controllers using different models for an experimental AMB system that contains flexible dynamics. They investigated the application of LPV control and gained scheduling via H_∞ controllers to an experimental AMB system [21]. An electromagnetic actuator based on passive vibration attenuation mechanism is installed on bearing in reference [22], and the two vibration attenuation types of constant current and pressure are analyzed. The electromagnetic actuator is designed to test the damping ratio of rotor system in reference [23]. These aforementioned methods need enough installation space of vibration control devices, and it is difficult for the high precision control of electromagnetic devices. Morosi and Santos [24] introduced the piezoactuator into a gas journal bearing to control the throttle parameters, and the vibration of the rotor was controlled actively. They had done theoretically and experimentally researches on the active lubrication bearing [25]. The linear and nonlinear control techniques were applied in actively lubricated journal bearings [26]. Simões et al. [27] used the piezoactuator to exert force on the rotor and control the vibration.

In this paper, a novel kind of hybrid bearing with the introduction of piezoelectric controller is proposed, and it has the function of control accuracy through static force method and dynamic force method. The principle of static force method and implementation of this hybrid bearing are researched. The basic structure characteristics of this bearing are that the tilting pads are set in the oil seal surface and there are piezoelectric ceramic transducer (PZT) components in the pivots of tilting pads. The radial position of tilting pad is changed by the elongation and shortening of PZT to adjust the preload coefficient, and then the rotor vibration is controlled.

2. Hybrid Bearing Scheme with the Introduction of Piezoelectric Controller

In this part, the new scheme of vibration control is proposed based on the analysis of vibration control technology, and then an example is given. This scheme can not only apply the static force method and dynamic force method but also implement the active control method of bearing vibration by using PZT component.

2.1. Vibration Control Technology. For high speed rotor bearing system, the general method of vibration control is improving the stiffness, which is defined as static force method. The optimization of structure or operational parameters can improve the stiffness of bearing that frequently used in the precision spindle system. For example, using film feedback throttle may obtain a very high stiffness [28]. Besides, tilting pad technology is introduced into hybrid bearing, in which the preload coefficient of tilting pad is adjusted by PZT, and then the bearing stiffness is improved. At the same time, the self-adapting tilting characteristic of tilting pad benefits the stability of bearing in high speed.

Another method of vibration control is dynamic force method, in which an opposite-direction dynamic force to the external exciting force is imposed on the rotor. Generally, this dynamic force is opposite to the unbalanced force, so the unbalanced force is counteracted to eliminate the unbalance response. For the precision spindle, a dynamic force opposite to the cutting force can also be imposed on the rotor to prevent the loss of accuracy in working condition. Then the precision remaining ability of spindle system is enhanced. The new kind of hybrid bearing proposed in this paper can adjust stiffness and impose dynamic preload. It has the function of vibration control through both static force method and dynamic force method. In this paper, only the model and simulation test of static force method are discussed.

2.2. Structure Module of New Bearing. The most important feature of this new bearing lies in the introduction of the piezoelectric control component that is set in the groove on oil seal surface of bearing. We can design the number and layout position of piezoelectric control components according to the working load and vibration condition of the rotor system. It is shown in Figure 1 that a piezoelectric control component is, respectively, set on the direction of left and right 45° of the upper bearing. In addition, the two piezoelectric control components can be set in the opposite directions, or we can set four piezoelectric control components in a bearing.

The function of piezoelectric control component is adjusting the clearance or preload coefficient of pad, and the structure is shown in Figure 2.

The PZT is installed in a cylindrical shell and is pretightened by a screw. A thrust ball bearing is set between the screw and PZT to prevent the rotation of PZT when tightening or loosing the screw. The force of PZT acted on the tilting pad via sensor base and pad base, between which a force sensor is set to test the force of PZT. The component is installed on the bearing pedestal. The clearance between pad and journal could be adjusted through turning the shell. A ball is set in the end of PZT to avoid the damage of PZT when the direction of loading force is misaligned with the axis of PZT.

2.3. Test and Control Module of New Bearing. For the vibration control method through adjusting preload coefficient
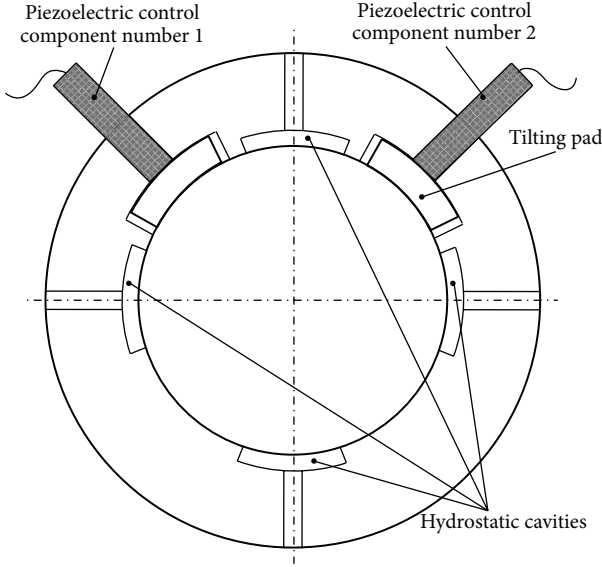
FIGURE 1: A structure scheme of new hybrid bearing.

FIGURE 2: Elements of piezoelectric control component.

FIGURE 3: Control schematic diagram of preload coefficient of new bearing.

of tilting pad in the abovementioned, the control schematic diagram is shown in Figure 3. The test and control system includes piezoelectric control component, controller, and displacement sensor. The PZT in this bearing should be driven by special controller, and the voltage signal is imported into PZT through the interface of controller.

There are two regulation modes of tilting pad clearance: (1) manual coarse tuning: turn the shell, and the space between pad and journal is changed; then the oil film stiffness will be adjusted; (2) automatic fine tuning. The displacement sensors are used to monitor the shaft vibration, and the vibration signals are imported into the controller. The needed stiffness of bearing could be calculated. The corresponding preload coefficient and driven voltage are acquired. Then the voltage signals are imported into PZT to control its elongation. The basic control process is shown in Figure 4.

3. Internal and External Characteristics of Piezoelectric Control Component

In this new bearing, the preload coefficient is automatically changed by elongation of PZT, and then the oil film stiffness is changed. But the elongation of PZT is not only related to the factory performance of PZT (called internal characteristic) but also influenced by oil film stiffness. In this paper, the preload coefficient control characteristic of PZT and oil film is called external characteristic.

3.1. Static Internal Characteristics of PZT. The fundamental feature of PZT is that its end elongates being electrified, and when the end is obstructed, the head will generate force, which is called activation force. The activation force is related to the design parameter of piezoactuator, such as piezoelectric coupling coefficient, piezoelectric constant, and the number of layers of piezoelectric material, and the nonlinear relationship exists between the voltage and
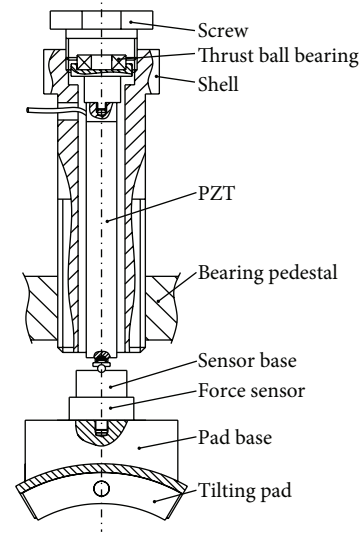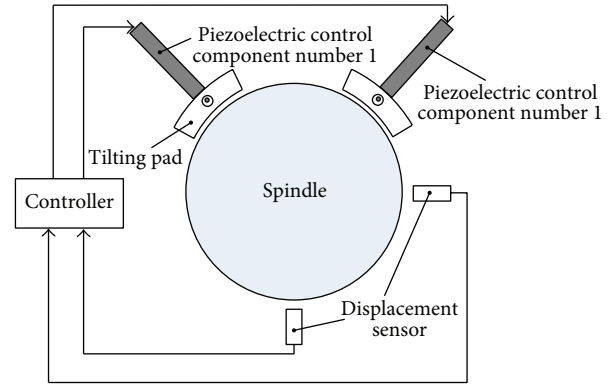
elongation. In this paper, the working range of PZT is small. The relationships among activation force, voltage, and elongation are simplified as linear [24], which is shown in Figure 5. When the driving voltage U (V) is maximum, the relationship between activation force F (N) and elongation x (μm) is shown as the red dashed line. When the elongation is always zero, the relationship between activation force and driving voltage is shown as the blue dash-dot line. When the activation force is always zero, the relationship between elongation and driving voltage is shown as the green solid line.

According to the above analysis, the model of activation force F_n in the linear working range is built, which can be described by two parameters [29]:

$$F_n = k_{n2}U - k_{n1}x, \tag{1}$$

where k_{n2} is the coefficient related to voltage (N/V), which is used to represent the electrical characteristics of PZT. k_{n1} is the coefficient related to displacement (N/μm), which is used to represent the mechanical characteristics of PZT. The two
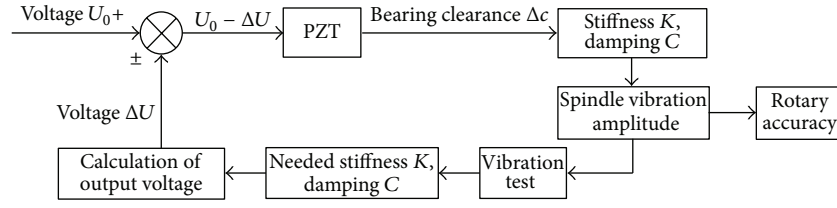
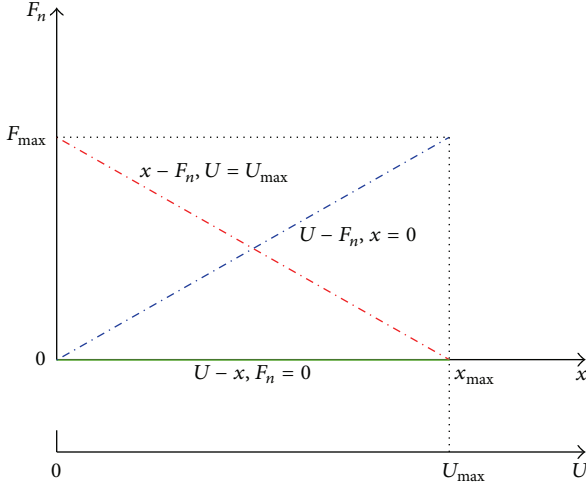FIGURE 4: Control process of bearing clearance.

FIGURE 5: Relationships among three parameters of PZT.

parameters characterize the static internal characteristics of piezoelectric control component.

3.2. Static External Characteristics of Piezoelectric Control Component.

The external characteristics of piezoelectric control component are related to the liquid film force. The mechanical model of PZT and bearing is shown in Figure 6.

The oil film forces acting on the shaft is considered as an elastic force because of the low damping of bearing, which can be described by stiffness k_y. The rotor is assumed to be a mass point. When the PZT is electrified, the end of PZT elongates and the activation force acting on liquid film causes the liquid film to be compressed at the same time. The elongation x of PZT is the displacement of the test point.

The stiffness k_y (N/μm) is the total stiffness of this new bearing with independent structure. It can be obtained by simple superposition of the stiffness of hydrostatic cavities k_j and the stiffness of tilting pads k_d. Consider

$$k_y = k_j + k_d. \tag{2}$$

According to [30], the stiffness of hydrostatic cavities is

$$k_j = \frac{12 P_s A_e (\beta - 1) \cos \theta_1}{h_0 \beta (2\beta - 1)}, \tag{3}$$

where P_s is the pressure of hydrostatic oil supply, θ_1 is the equivalent cornerite of oil chamber, A_e is the effective bearing area, h_0 is the radial clearance of hydrostatic cavities, and β is throttle pressure ratio of orifice-type restrictor [31].

The stiffness of tilting pads is calculated by solving the Reynolds Equation [32]:

$$\frac{\partial}{\partial x} \left(h^3 \frac{\partial p}{\partial x} \right) + \frac{\partial}{\partial y} \left(h^3 \frac{\partial p}{\partial y} \right) = 6 U \eta \frac{\partial h}{\partial x}, \tag{4}$$

where U is the circumferential speed of the journal and η is the lubricating oil viscosity. p is the oil film pressure, which can be solved numerically by Finite Difference Method (FDM). Then the static and dynamic characteristics of tilting pads can be acquired, including oil film thickness and stiffness k_d.

Then the relational expressions are as follows:

$$F_n = k_{n2} U - k_{n1} x$$
$$F_n = k_y x. \tag{5}$$

The above expressions can be converted to

$$F_n = \frac{k_y k_{n2} U}{k_y + k_{n1}}$$
$$x = \frac{k_{n2} U}{k_y + k_{n1}}. \tag{6}$$

Actually, because of the spaces between each component after assembly, the piezoelectric control component needs to be pretightened. The mechanical model is shown in Figure 6(b). It is supposed that the PZT of Δ_1 is compressed by a pretightening force F_0. The fluid film of Δ_2 is compressed. x is the displacement of the test point. The relational expressions are as follows:

$$F_n = k_{n2} U - k_{n1} (x - \Delta_1)$$
$$F_n = k_y (x + \Delta_2) \tag{7}$$
$$F_0 = k_{n1} \Delta_1 = k_y \Delta_2.$$

Similarly, the above expressions can be converted to the following:

$$F_n = \frac{k_y k_{n2} U}{k_y + k_{n1}} + F_0$$
$$x = \frac{k_{n2} U}{k_y + k_{n1}}. \tag{8}$$

The preload coefficient of tilting pad can be adjusted by the stretch of PZT. The geometrical relationship of pad and

(a) Without pretightening force
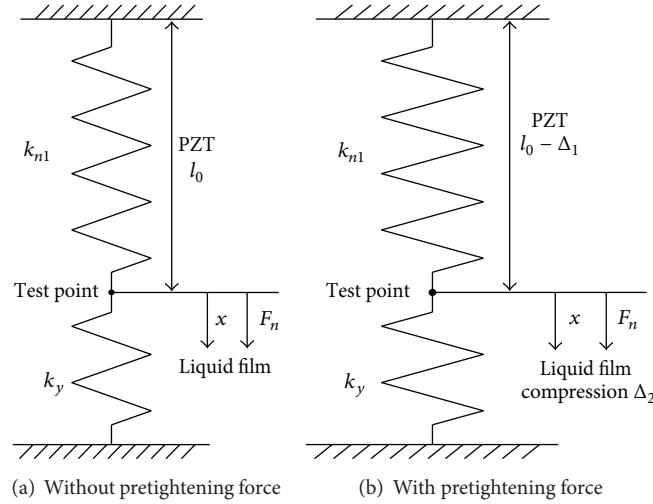
(b) With pretightening force

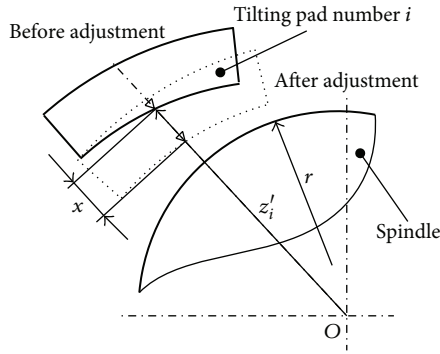Figure 6: Mechanical models of PZT and bearing.

Figure 7: Geometrical relationship diagram of adjusting of preload coefficient.

journal is shown in Figure 7. It is supposed that the elongation of PZT is x, the distance between pivot of i# tilting pad and centroid of journal is z_i', and then $z_i' = R - x$, where R is the radius of curvature of tilting pad which is supposed to be initial distance. The relational expression between preload coefficient of tilting pad and elongation of PZT is as follows:

$$m = 1 - \frac{c_1}{c_2} = 1 - \frac{z_i' - r}{R - r} = \frac{x}{R - r}, \tag{9}$$

where c_1 is installation clearance (μm), which is related to the pivot position of tilting pad after installation, and $c_1 = z_i' - r$. r is the radius of journal. c_2 is machining gap (μm), which is related to the radius of curvature of tilting pad surface in processing, and $c_2 = R - r$.

When the elongation of PZT is zero, the preload coefficient is zero. Substitute (8) into (9), and calculation equation of preload coefficient of the new bearing is obtained, which shows that the preload coefficient is not only related to the geometric parameters of bearing but also affected by the oil film stiffness and internal characteristics of PZT. Besides, there are certain relationships between preload coefficient and oil film stiffness under hydrodynamic effects. The

coupled relationships determine that the preload coefficient should be adjusted accurately during the running of bearing. Of course, it also can be adjusted roughly by the simulated relationship between preload coefficient and stiffness when the machine is shut down.

4. Simulation Experiment on Adjusting and Controlling of Bearing's Preload Coefficient

According to the above analysis, it is known that the adjustment of preload coefficient is related to the oil film stiffness and internal characteristics of PZT. Equation (6) is given based on supposition that the relationships among activation force, voltage, and elongation are linear. So it is necessary to set simulated experiment to verify the supposition and amend the internal characteristic coefficients.

4.1. Experimental Setup. The experimental setup is shown in Figure 8. An orthogonal top cover is designed to install the piezoelectric control component, which can ensure that the axis of piezoelectric control component is overlapped with 45° line of shaft. The fixed pad is slot with two grooves on the direction of $\pm 45°$, in which disc spring components are set to simulate the stiffness of oil film. Because the functions of two PZT are superposed, just one PZT is used in the simulation test, which do not affect the test results.

The piezoactuator elongates when the electric current is applied on the piezoelectric control component by a signal generator; then the forces of piezoactuator act on the spindle. The spring under the spindle is compressed. The spindle moves in the direction of activation force. The stiffness of disc spring components is 10^6 N/m order of magnitude. An eddy current sensor is set on the direction of activation force to measure the displacement of the spindle. The force of piezoactuator is measured by the force sensor set between the tilting pad and the bearing base.

The type of PZT used in this test is PSt150/14/140VS20, and controller of XE-501c is equipped. The factory parameters

(a) Structure diagram
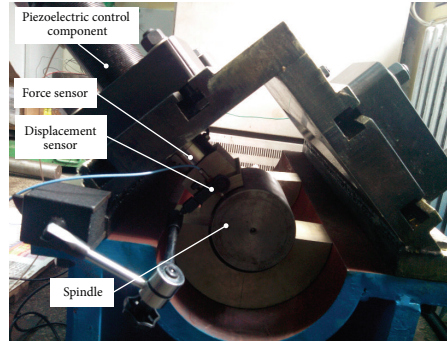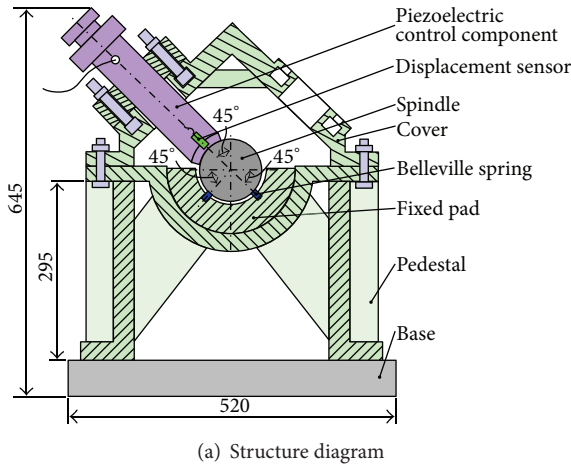
(b) Photo of experimental setup

FIGURE 8: The experimental setup and photo of simulation experiment on preload coefficient.
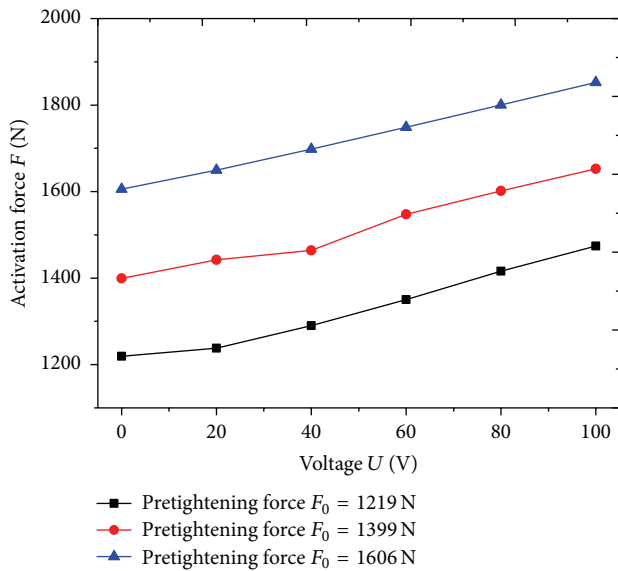

FIGURE 9: Activation force versus driven voltage under different pretightening forces.

are as follows: the initial length $l_0 = 143$ mm, the maximum driven voltage is 150 V, the rated activation force is 7000 N, and the rated stroke is 140 μm. So, for this PZT, the nominal values of coefficients in (1) are as follows: $k_{n1} = 50$ N/μm and $k_{n2} = 46.7$ N/V.

4.2. Amendment of External Characteristic Coefficients of Piezoelectric Control Component.
In order to analyze the influence of pretightening force on external characteristics of piezoelectric control component, the relationships between activation force and voltage under three different pretightening forces are acquired from the test data on the test bench, which is shown in Figure 9. Different pretightening forces are implemented on the piezoactuator, and the activation forces under different driven voltages are tested and recorded. The activation forces are basically linearly increasing with

the increasing of driven voltage, and the slopes of three lines are almost equal. The impact of pretightening force on the external characteristics of piezoelectric control component is quite small. At the same time, it is shown that the coefficient related to voltage k_{n2} is constant, which verifies the above linear supposition.

When the pretightening force is 1606 N, the activation forces, displacements, and driven voltages are tested under three different kinds of stiffness of disc spring components, which are shown in Figure 10. The stiffness of the three disc spring components is, respectively, 3.7 N/μm, 3.9 N/μm, and 5.4 N/μm. The activation forces are calculated by subtracting the pretightening force from the data of force sensor. It is shown that the activation forces and displacement are basically linearly increasing with the increasing of driven voltage, and the slopes of three lines are related to the simulated stiffness. According to (6), the activation forces and displacement are nonlinear with the simulated stiffness, so the activation forces and displacement do not increase with the simulated stiffness under the same voltage.

In practice, because of the operational condition and assembly, the mechanical characteristics of piezoelectric controller will probably be changed. We can amend k_{n1} using the test data of the simulated stiffness 3.9 N/μm, and k_{n1} is amended to 72.5 N/μm. Then the amended theoretical values are calculated by (6) with the emendation of k_{n1}. The nominal values are calculated by (6) with the nominal value of k_{n1} and k_{n2} (50 N/μm). The experimental values are the test data when the stiffness of disc spring was 3.9 N/μm. The comparison among the nominal value, experimental value, and amended theoretical value is shown in Figure 11. It is seen that the amended theoretical value is closer to the experimental value.

4.3. Open-Loop Adjustment of Bearing Preload Coefficient.
For a certain grinding spindle, an example of bearing is designed, and the parameters of hydrostatic cavity and tilting pad are shown in Tables 1 and 2. The structural style of this bearing is four cavities and orifice throttle. A piezoelectric control component is set in each oil seal surface, and then

(a) Activation force versus displacement

(b) Activation force versus driven voltage
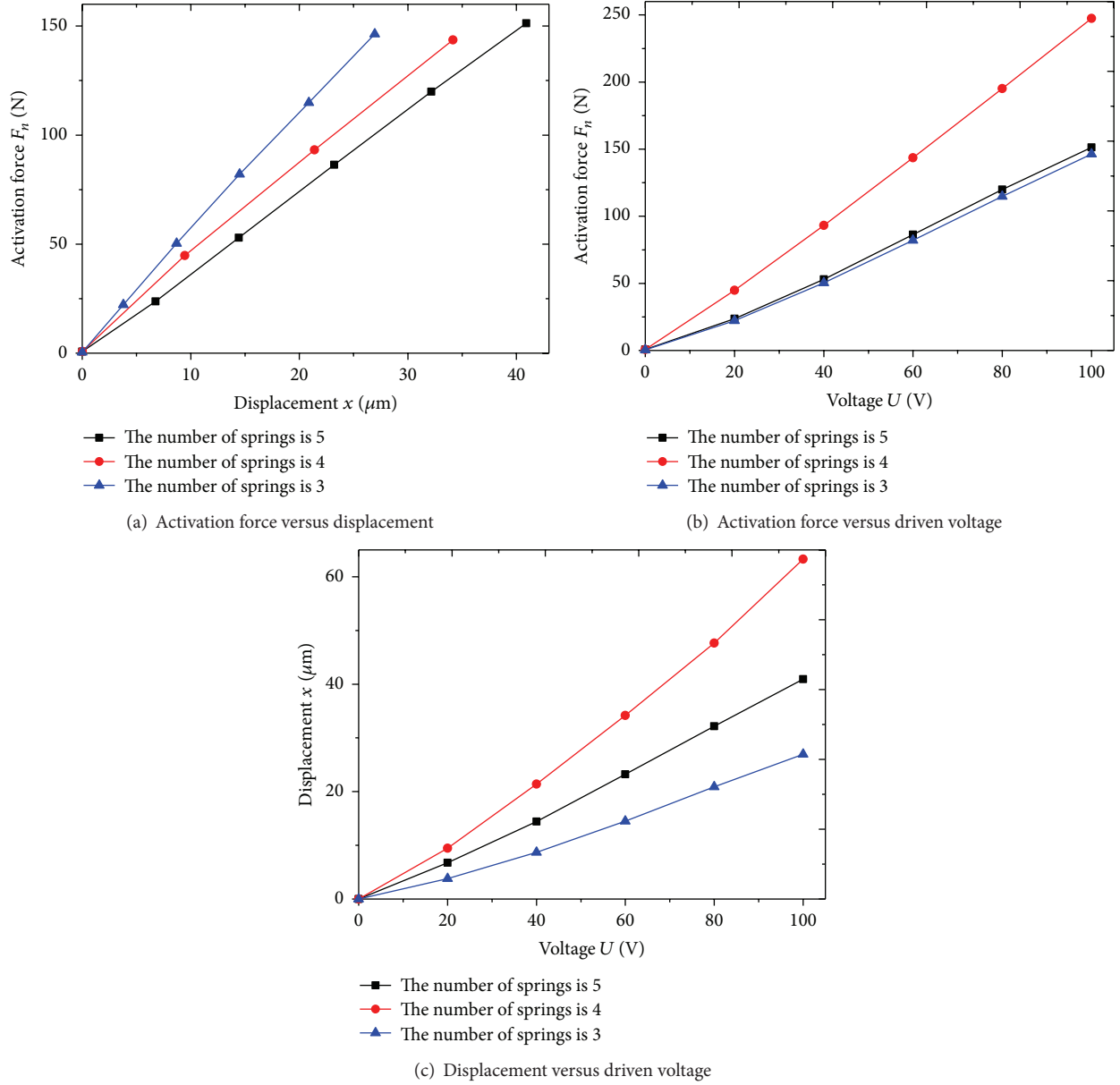

(c) Displacement versus driven voltage

Figure 10: Relationships among activation force, displacement, and driven voltage under different simulated stiffness.

the new bearing with four hydrostatic cavities and four tiling pads is constituted.

Firstly, the oil film stiffness of the bearing under different radial clearances and preload coefficients are obtained by solving Reynolds Equation (4), which is shown in Figure 12. When the piezoactuators are used for controlling the preload coefficients of tilting pads, the displacements of piezoactuators can be calculated by (9). Then the relationship between preload coefficients and driven voltages are derived from (6) with the amended value of k_{n1}. So the preload coefficients can be controlled by adjusting the driven voltages according to Figure 13. It is seen that the driven voltage of PZT has a significant regulatory effect on the preload coefficient. For the bearing studied in this paper, when the preload coefficient is less than 0.3, the regulatory abilities of driven

voltage on preload coefficient under different radial gaps are basically identical. The reason is that the stiffness of different radial gaps changes a little in small preload coefficients and the driven voltages used to conquer film force are near. If more data in bigger range is calculated according to the possible vibration condition and amended by experiment, the amended data can be used for open-loop adjustment of bearing preload coefficient of this new bearing. The voltage is adjusted based on the monitoring data of activation force of PZT to control the preload coefficient of bearing.

5. Conclusions

In this paper, a kind of hybrid bearing with the introduction of piezoelectric controller is proposed. The internal and

(a) Displacement and driven voltage

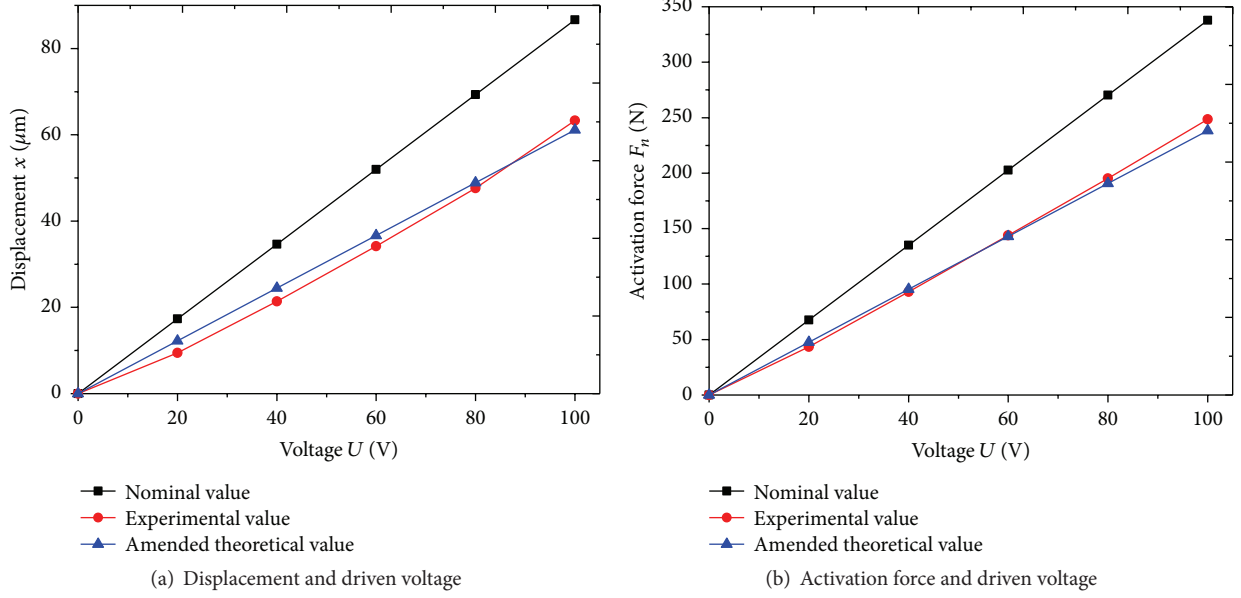(b) Activation force and driven voltage

FIGURE 11: Comparison among the nominal values, experimental values, and amended theoretical values.
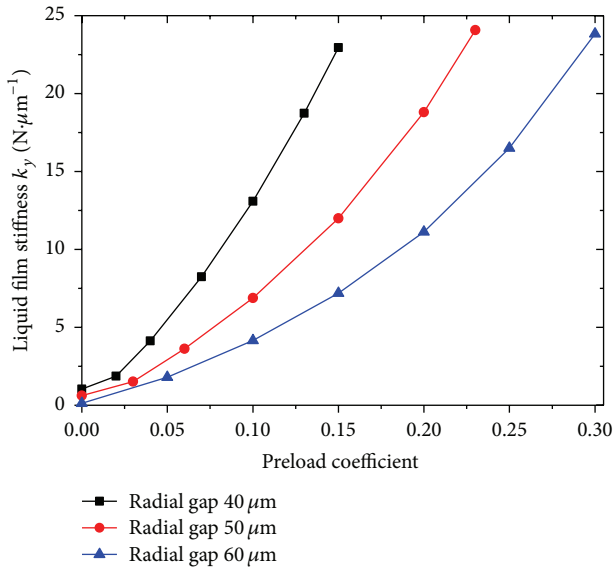

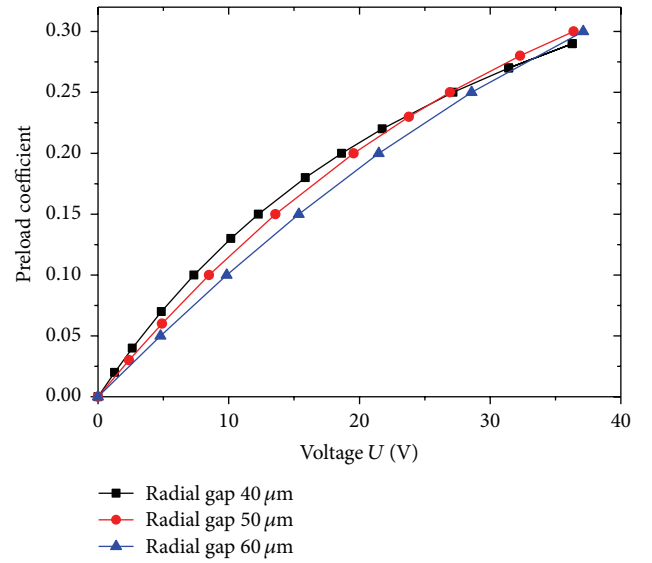FIGURE 12: Relationships between oil film stiffness and preload coefficient under different radial gaps.

FIGURE 13: Relationship between preload coefficient and driven voltage under different radial gaps.

external characteristics are analyzed, and simulation test is carried out. The main conclusions are as follows:

(1) The structure scheme of hybrid bearing with the introduction of piezoelectric controller and tilting pad is proposed. The new bearing can adjust the preload coefficient of tilting pad actively.

(2) The static internal characteristics of PZT and static external characteristics of piezoelectric control component are analyzed. The calculation equations of preload coefficient and activation force of the new bearing are given. The adjustment capacity of preload

coefficient is limited by the oil film stiffness and internal characteristics of PZT.

(3) The experimental setup of this new bearing is designed and developed. The relationships among displacement of pivot, activation force, driven voltage, and oil film stiffness are obtained. It is verified that the relationships among activation force, voltage, and elongation are linear. The nominal internal characteristic coefficients of PZT are amended by test data, and the influence of driven voltage on preload coefficient under different radial gaps of bearing is analyzed.

TABLE 1: Parameters of structure and operating conditions of hydrostatic cavities.

Parameter item	Symbol	Unit	Value
Diameter of bearing	D	mm	100
Width of bearing	L	mm	100
Radial gap of hydrostatic cavity	c	μm	40–60
Axial width of oil seal surface	l_1	mm	12
Circular width of oil seal surface	b_1	mm	3
Cornerite of hydrostatic cavity	$2\theta_1$	°	11
Cornerite of hydrostatic cavity and oil seal surface	$2\theta_2$	°	18
Orifice diameter of small orifice-type restrictor	d_0	mm	1
Rated load	W	N	100
Rated speed	n	r/min	10000
Supply pressure	P_s	MPa	2

TABLE 2: Structure parameters of tilting pads.

Parameter item	Symbol	Unit	Value
Diameter of bearing	D	mm	100
Width of tilting pads	L_d	mm	50
Radial gap of tilting pads	c_1	μm	40–60
Preload coefficient	m		0–0.3
Number of pads	Z		4
Cornerite of tilting pad	θ	°	50

Competing Interests

The authors declare that they have no competing interests.

Acknowledgments

References

[1] S. C. Sharma, S. C. Jain, R. Sinhasan, and R. Shalia, "Comparative study of the performance of six-pocket and four-pocket hydrostatic/hybrid flexible journal bearings," *Tribology International*, vol. 28, no. 8, pp. 531–539, 1995.

[2] F. Xue, W. H. Zhao, Y. L. Chen, and Z. W. Wang, "Research on error averaging effect of hydrostatic guideways," *Precision Engineering*, vol. 36, no. 1, pp. 84–90, 2012.

[3] C. H. Song, "Status and developing trend of NC technology," *Equipment Manufacturing Technology*, no. 3, pp. 114–117, 2011.

[4] L. Wang, S. Y. Pei, X. Z. Xiong, and H. Xu, "Study on the static performance and stability of a water-lubricated hybrid bearing with circumferential grooves and stepped recesses considering the influence of recess sizes," *Tribology Transactions*, vol. 57, no. 1, pp. 36–45, 2013.

[5] L. San Andres, D. Childs, and Z. Yang, "Turbulent-flow hydrostatic bearings: analysis and experimental results," *International Journal of Mechanical Sciences*, vol. 37, no. 8, pp. 815–829, 1995.

[6] L. Guo, "Different geometric configurations research of high speed hybrid bearings," *Journal of Human University of Arts and Science*, vol. 15, no. 3, pp. 40–43, 2003.

[7] N. Singh, S. C. Sharma, S. C. Jain, and S. S. Reddy, "Performance of membrane compensated multirecess hydrostatic/hybrid flexible journal bearing system considering various recess shapes," *Tribology International*, vol. 37, no. 1, pp. 11–24, 2004.

[8] A. van Beek and R. A. J. van Ostayen, "Analytical solution for tilted hydrostatic multi-pad thrust bearings of infinite length," *Tribology International*, vol. 30, no. 1, pp. 33–39, 1997.

[9] N. Heinrichson, I. F. Santos, and A. Fuerst, "The influence of injection pockets on the performance of tilting-pad thrust bearings—part I: theory," *Transactions of the ASME, Journal of Tribology*, vol. 129, no. 4, pp. 895–903, 2007.

[10] N. Heinrichson, A. Fuerst, and I. F. Santos, "The influence of injection pockets on the performance of tilting-pad thrust bearings—part II: comparison between theory and experiment," *Journal of Tribology*, vol. 129, no. 4, pp. 904–912, 2007.

[11] X. Raud, M. Fillon, and M. Helene, "Numerical modelling of hydrostatic lift pockets in hydrodynamic journal bearings—application to low speed working conditions of highly loaded tilting pad journal bearings," *Mechanics and Industry*, vol. 14, no. 5, pp. 327–334, 2013.

[12] X. Z. Wang, X. Y. Yuan, J. Zhu, and D. M. Qiu, "Research on the pivot structure of hybrid tilting-pad journal bearing," *Manufacturing Technology & Machine Tool*, no. 6, pp. 24–26, 1997.

[13] X. Z. Wang, X. Y. Yuan, J. Zhu, D. M. Qiu, and W. Shihu, "Test and analysis on the system damping of the hybrid tilting-pad journal bearing," *Mechanical Science and Technology*, vol. 15, no. 5, pp. 721–724, 1996.

[14] S.-Y. Liu, Z.-H. Xiao, Z.-Y. Yan, and Z.-J. Chen, "Vibration characteristics of rotor system with tilting-pad journal bearing of elastic and damped pivots," *Journal of Central South University*, vol. 22, no. 1, pp. 134–140, 2015.

[15] T. G. Choi and T. H. Kim, "Analysis of tilting pad journal bearings considering pivot stiffness," *Journal of the Korean Society of Tribologists and Lubrication Engineers*, vol. 30, no. 2, pp. 77–85, 2014.

[16] Z. Yan, Y. Lu, and T. Zheng, "An analytical complete model of tilting-pad journal bearing considering pivot stiffness and damping," *Journal of Tribology-Transactions of the ASME*, vol. 133, no. 1, Article ID 011702, 2011.

[17] Y. Kang, T. W. Lin, M. H. Chu, Y. P. Chang, and Y. P. Wang, "Design and simulation of a neural-PD controller for automatic balancing of rotor," in *Advances in Neural Networks—ISNN 2006, PT 2, Proceedings*, vol. 3972, pp. 1104–1109, Springer, 2006.

[18] F.-Z. Hsiao, C. Chue-Fan, W.-H. Chieng, and A.-C. Lee, "Optimum magnetic bearing design considering performance limitations," *JSME International Journal, Series C: Dynamics, Control, Robotics, Design and Manufacturing*, vol. 39, no. 3, pp. 586–596, 1996.

[19] Y. Suzuki, "Acceleration feedforward control for active magnetic bearing systems excited by ground motion," *IEE Proceedings—Control Theory and Applications*, vol. 145, no. 2, pp. 113–118, 1998.

[20] H. M. N. K. Balini, C. W. Scherer, and J. Witte, "Performance enhancement for AMB systems using unstable H_∞ controllers," *IEEE Transactions on Control Systems Technology*, vol. 19, no. 6, pp. 1479–1492, 2011.

[21] H. M. N. K. Balini, J. Witte, and C. W. Scherer, "Synthesis and implementation of gain-scheduling and LPV controllers for an AMB system," *Automatica*, vol. 48, no. 3, pp. 521–527, 2012.

[22] S. W. Dyer, *Adaptive Optimal Control of Active Balancing Systems for High-Speed Rotating Machinery*, University of Michigan, Ann Arbor, Mich, USA, 1999.

[23] S. Ma, S. Pei, L. Wang, and H. Xu, "A novel active online electromagnetic balancing method-principle and structure analysis," *Transactions of the ASME Journal of Vibration and Acoustics*, vol. 134, no. 3, Article ID 034503, pp. 1–8, 2012.

[24] S. Morosi and I. F. Santos, "Active lubrication applied to radial gas journal bearings—part 1: modeling," *Tribology International*, vol. 44, no. 12, pp. 1949–1958, 2011.

[25] I. F. Santos and A. Scalabrin, "Control system design for active lubrication with theoretical and experimental examples," *Journal of Engineering for Gas Turbines and Power*, vol. 125, no. 1, pp. 75–80, 2003.

[26] R. Nicoletti and I. F. Santos, "Linear and non-linear control techniques applied to actively lubricated journal bearings," *Journal of Sound and Vibration*, vol. 260, no. 5, pp. 927–947, 2003.

[27] R. C. Simões, V. Steffen Jr., J. Der Hagopian, and J. Mahfoud, "Modal active vibration control of a rotor using piezoelectric stack actuators," *Journal of Vibration and Control*, vol. 13, no. 1, pp. 45–64, 2007.

[28] Y. S. Chen, *Theory and Design of Hydrostatic Bearing*, National Defence Industry Press, Beijing, China, 1980.

[29] Z. Zhang, M. Xu, B. Feng, and X. Zhang, "A round-trip piezoelectric actuator with variable step and large displacement," *Chinese Journal of Applied Mechanics*, vol. 27, no. 1, pp. 108–112, 2010.

[30] H. Zhong and G. K. Zhang, *Design Manual of Hydrostatic and Hybrid Bearings*, Electronic Industry Press, Beijing, China, 2007.

[31] Z. H. Pang and S. J. Chen, *Liquid Hydrostatic and Hybrid Bearings*, Harbin Institute of Technology Press, Harbin, China, 1991.

[32] Z. M. Zhang, *Hydrodynamic Lubrication Theory of Sliding Bearing*, Higher Education Press, Beijing, China, 1986.